Saudi Pharmaceutical Journal 32 (2024) 101889

HOSTED BY

Contents lists available at ScienceDirect

Saudi Pharmaceutical Journal

journal homepage: www.sciencedirect.com

Molecular docking, drug-likeness and DFT study of some modified tetrahydrocurcumins as potential anticancer agents

Ahmed Mahal [a,*], Marwan Al-Janabi [b], Volkan Eyüpoğlu [b], Anas Alkhouri [j], Samir Chtita [c], Mustafa M. Kadhim [d,e], Ahmad J. Obaidullah [f], Jawaher M. Alotaibi [f], Xiaoyi Wei [g,h], Mohammad Rizki Fadhil Pratama [i]

[a] Department of Medical Biochemical Analysis, College of Health Technology, Cihan University-Erbil, Erbil, Kurdistan Region, Iraq
[b] Department of Chemistry, Çankırı Karatekin University, Çankırı, Turkey
[c] Laboratory of Analytical and Molecular Chemistry, Faculty of Sciences Ben M'Sik, Hassan II University of Casablanca, Casablanca, Morocco
[d] Department of Dentistry, Kut University College, Kut, Wasit 52001, Iraq
[e] Medical Laboratory Techniques Department, Al-Farahidi University, Baghdad, 10022, Iraq
[f] Department of Pharmaceutical Chemistry, College of Pharmacy, King Saud University, P.O. Box 2457, Riyadh 11451, Saudi Arabia
[g] Laboratory of South China Agricultural Plant Molecular Analysis and Genetic Improvement and Guangdong Provincial Key Laboratory of Digital Botanical Garden and Public Science, South China Botanical Garden, Chinese Academy of Sciences, Xingke Road 723, Tianhe District, Guangzhou 510650, People's Republic of China
[h] University of Chinese Academy of Sciences, Yuquanlu 19A, Beijing 100049, People's Republic of China
[i] Department of Pharmacy, Universitas Muhammadiyah Palangkaraya, Palangka Raya, Central Kalimantan 73111, Indonesia
[j] College of Pharmacy, Cihan University-Erbil, Erbil, Kurdistan Region, Iraq

ARTICLE INFO

Keywords:
Tetrahydrocurcumin
Docking
DFT
ADMET
Anticancer

ABSTRACT

The present study utilized molecular docking and density functional theory (DFT) approaches, and ADMET (absorption, distribution, metabolism, excretion, and toxicity) properties to investigate the binding interactions, reactivity, stability, and drug-likeness of curcumin (1), tetrahydrocurcumin (2), and tetrahydrocurcumin derivatives (3–6) as potential anti-cancer agents. MGL (Molecular Graphic Laboratory) and Discovery Studio Visualizer (DSV) software employed for docking studies. Pharmacokinetic and pharmacodynamic (ADME-Tox) analyses were conducted using SwissADME and pKCSM web servers. Total Electron Density (TED) measurements identified molecular adsorption sites, considering various factors, including quantum chemical characteristics, to assess compound effectiveness using DFT method implanted in the Gaussian software. The binding energy (Eb) from docking simulations was used to evaluate inhibitory potential. ADMET analysis suggested favorable oral bioavailability and pharmacokinetics for all studied substances, excluding compound 4. DFT and docking investigations highlighted compounds 1, 2, and 6 as optimal scaffolds for drug design based on in silico screening tests.

1. Introduction

Plants paly important role as medicines for long time (Fridlender et al., 2015). Plant-derived substance including paclitaxel (Wani et al., 1971), cannabinoids (Velasco et al., 2015) and curcumin. Curcumin is a phytochemical of the Zingiberaceae family isolated from the rhizome of turmeric Curcuma longa (Lakhan et al., 2015). Turmeric that contains 2 % to 5 % curcumin is a result of the treatment of the rhizome or root (Wilken et al., 2011). The three major structures of turmeric extract are curcumin (1, 60–70 %), demethoxycurcumin (2, 20–27 %), and bisdemethoxycurcumin (4, 10–15 %), along with other few secondary metabolites as shown in Fig. 1 (Nelson et al., 2017). Curcuma longa species are forming bright yellow curcumin. Curcumin is used in the market as herbal medicine, food flavoring, coloring agents, and cosmetics ingredient. A diarylheptanoid of curcumin that belongs to the curcuminoids family of phenolic pigments that give turmeric its yellow color. Although a lot of studies done but investigating no evidence for its therapeutic activity due to its both instability and poor bioavailability and therefore, it is unlikely to be drug development (Baker, 2017, Manolova et al., 2014).

The reduction of curcumin (Pari et al., 2005) leads to the production of another curcuminoid of turmeric so called tetrahydrocurcumin (THC)

* Corresponding author.
E-mail address: ahmed.mahal@cihanuniversity.edu.iq (A. Mahal).

https://doi.org/10.1016/j.jsps.2023.101889
Received 15 October 2023; Accepted 30 November 2023
Available online 1 December 2023

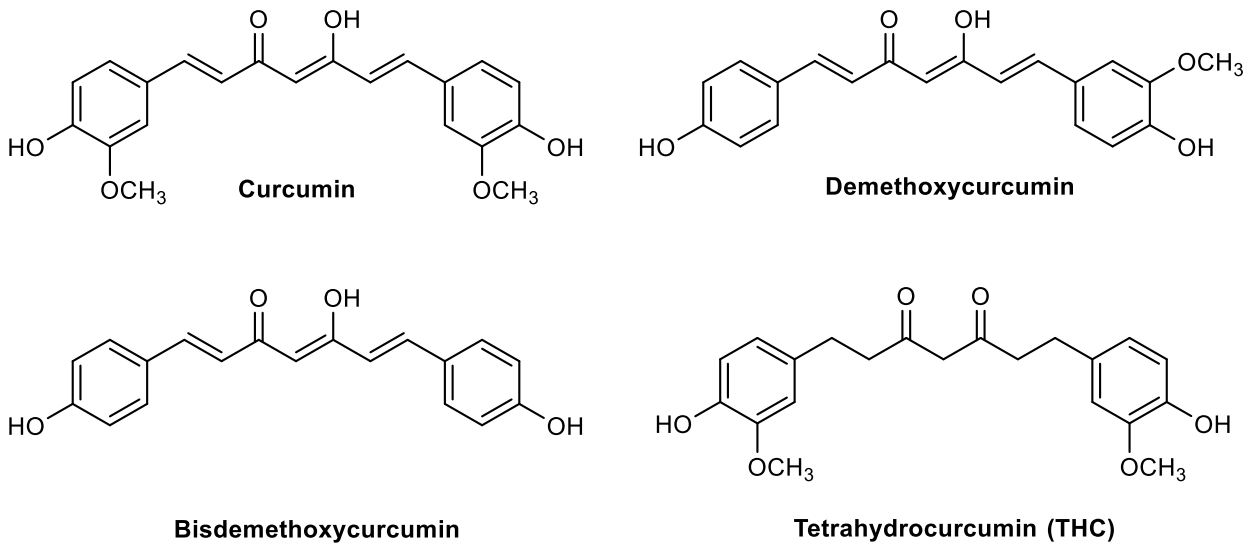

Fig. 1. The major structures of turmeric extracts of including curcumin, demethoxycurcumin, bisdemethoxycurcumin and tetrahydrocurcumin.

(Fig. 1) which is isolated from Curcuma wenyujin (Song et al., 2018) as traditional Chinese medicine. Phase I metabolism is producing THC by hepatic reductases as a curcumin major metabolite (Esatbeyoglu et al., 2012). On the other hand, the hydrogenation of curcumin is producing THC (white color) in the laboratory and investigated its bioactivity as an anti-inflammatory, antioxidant, and anticancer agent (Karthikesan et al., 2010, Kim et al., 2021, Li et al., 2021, Song et al., 2018, Zhao et al., 2015). The findings show the potent cytotoxic activity of THC as anti-cancer agents (Duan et al., 2022; Mahal et al., 2019, 2017) and as an cancer chemoprevention (Kim et al., 1998). THC shows the potent inhibitory activity as P-glycoprotein (P-gp) inhibitors against multidrug resistance in the cancer diseases (Limtrakul et al., 2007). In-silico study was used an effective tool to search for search for new drugs especially from plants (Aanouz et al., 2021, Chen and Nakamura, 2004, Soudani et al., 2023, El Khatabi et al., 2023). To develop better treatment against cancer and in order to examine the potential of curcumin compounds as anticancer medicines, Saeed and coworkers employ a technique known as molecular docking to target the cancer-related target proteins of curcumin, including EGFR and nuclear factorκB (NF-κB) (Saeed et al., 2022). Additionally, they used the annexin V/propidium iodide assay, lactate dehydrogenase assay, reassuring cell viability assay, and flow cytometry measurement of reactive oxygen species to validate the docking results for locating a curcumin-based drug against cancer. Performed molecular docking to show that potential of twenty-two selected food-derived compounds as hyperglycemia reducers. They found that curcumin is a dual inhibitor of DPP-4 and α-glucosidase, two enzymes important for glycemic control. Based on the docking results, they examined the enzymatic evaluation via in vitro studies. Cao and coworkers discovered that curcumin dramatically alleviated the diet-induced hyperglycemia in mice. This condition was brought on by a change in the mice's diet. Curcumin is highlighted as a potential component of foods with functional qualities that are utilized to manage diet-induced hyperglycemia in a study that was investigated by Cao and coworkers (Cao et al., 2022). The DFT analyses of synthesized curcumin analogues were studied by Ahsan and coworkers (Ahsan et al., 2022), where the HOMO/LUMO configuration of the compounds lies between the energy levels E = 3.55 and 3.35 eV. In addition, the anti-proliferative efficiency of curcumin analogues was evaluated using a total of fifty dozen distinct cancer cell lines in both a single dosage experiment (10 M) and five dose assays (0.001 to 100 M). Among the prepared compounds, two derivatives demonstrated the most encouraging anti-proliferative activity against the cancer cell lines, with growth inhibitions of 92.41 % and 87.28 %, respectively. In addition to this, it demonstrated significant antiproliferative activity (%GIs > 68 %) against fifty-four of the use of curcumin analogues as a therapeutic intervention may prove to be advantageous in the fight against cancer, as suggested by the findings of Ahsan and coworkers (Ahsan et al., 2022). In an investigation into the inhibition of aldose reductase (rate-limiting enzyme of progression of diabetic complications), Kondhare and coworkers synthesized of novel series of curcumin analogues and biological activity studies implemented (Kondhare et al., 2019). The biological activity revealed that, in comparison to the quercetin standard, all curcuminoids have androgen receptor inhibitory (ARI) activities that ranged from moderate to good. They reported that five compounds of newly synthesized have IC_{50} values less than 5.95 μM. In our continuous attempts to develop novel potent bioactive agents (Abdel-Jalil et al., 2015; El-Barasi et al., 2020; El-ajaily et al., 2019; Eleya et al., 2011; Hussain et al., 2008; Ibad et al., 2011; Kamel et al., 2022a, 2022b; Mahal, 2015a; Mahal et al., 2010, 2011, 2015a,b, 2019, 2021; Marzano et al., 2022; Mohapatra et al., 2021; Salman et al., 2011, 2020, 2022, Yang et al., 2017, 2018, Zinad et al., 2021a,a,b,b–d, 2022, 2023a,b), we aim at this study to investigate the molecular docking and DFT calculation of potent anticancer agents of tetrahydrocurcumin.

2. Materials and methods

2.1. Cytotoxic activity assay

The cytotoxic activity assay was performed according to the previous procedure (Mahal et al., 2017).

2.2. Calculation methods

2.2.1. Ground state predictions

Fig. 2 shows the anticancer inhbitory activity of the THC and its derivativess. Gaussian 09 was utilized in conjunction with DFT calculations (Plata and Singleton, 2015). The 6-311G* basis set and the B3LYP as the exchange–correlation funcional were used (Salman et al., 2019). The energy of the highest occupied molecular orbital (EHOMO), the energy of the lowest unoccupied molecular orbital (ELUMO), Egap = EHOMO- ELUMO, global hardness (η), global softness (η), electrophilicity index (ω), and dipole moment (μ) were computed, among other chemical parameters (Lee et al., 1988).

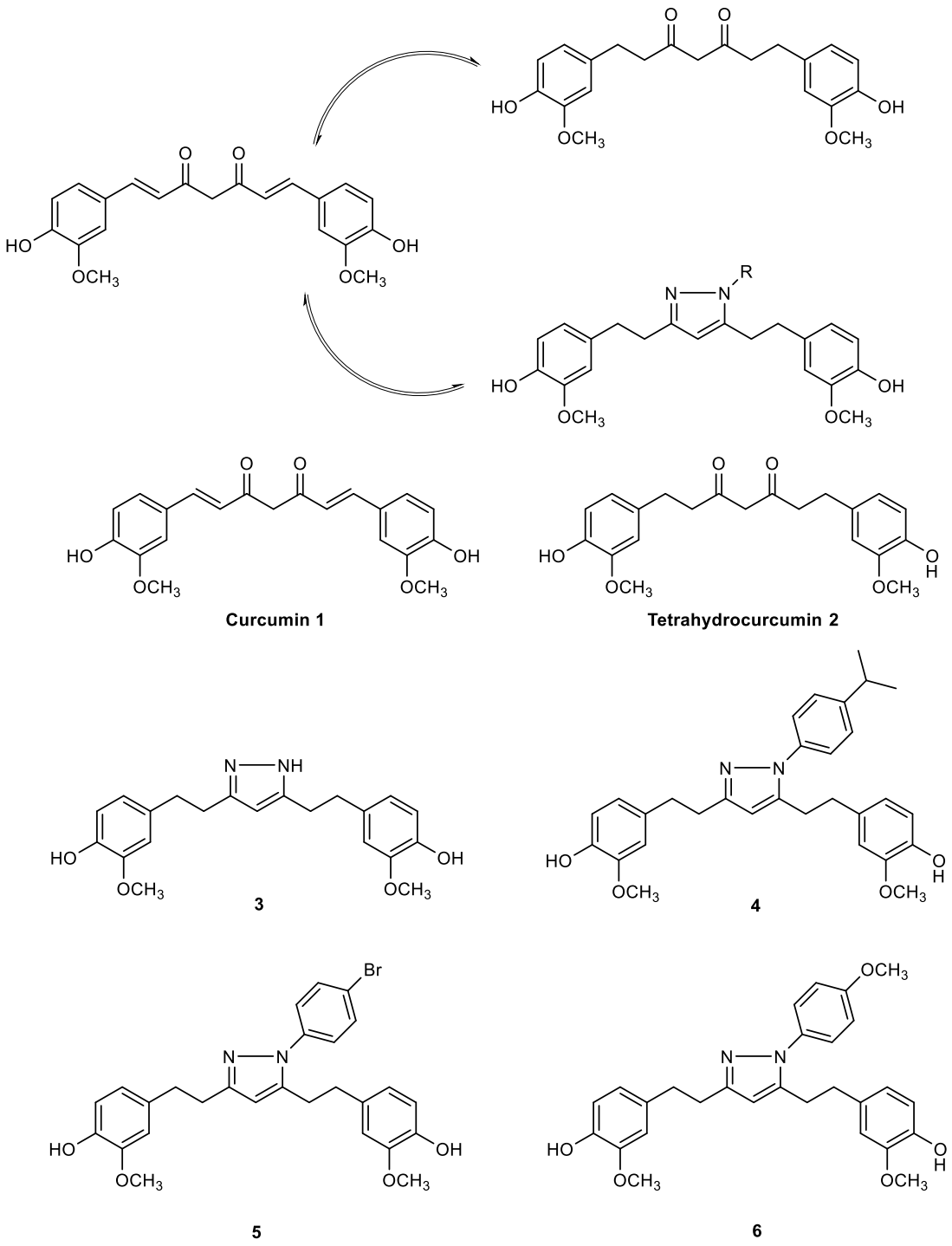

Fig. 2. The basic mechanisms and 2D structures for the study of compounds (1–6).

2.2.2. Physical properties

2.2.2.1. Charge of the atom. Electrostatic (polar) or orbital cooperation in chemistry (covalent). Electrostatic collaboration is made possible by the presence of electric charges inside the particle. Many chemical reactions and the physical characteristics of substances are influenced by the local electron density or charge density. The densities of local electrons or charges are necessary and respond to the physical and chemical properties of compounds. Along these lines, depending on the parameters of charge for measuring molecular activity. As an outcome, there are numerous techniques for calculating the partial charges. Mulliken populace investigation was utilized for the count of the charge distribution in a particle. In addition, the subatomic polarity is described using atomic charges (Sayin et al., 2019).

2.2.2.2. Orbital energies of the molecule. The highest occupied molecular orbital energy (EHOMO) is the orbital that has an electron to contribute to bonds. On the other hand, the lowest unoccupied molecular orbital energy (ELUMO) is the deepest (lowest energy) orbital that may take electrons, making it a potential electron acceptor. According to the border molecular orbital theory, the interaction between the two orbitals (HOMO and LUMO) of reactants determines the structure of a

transition state. The design of a transition state is the result of this collaboration (Radhi et al., 2020). Both the ionization potential of the HOMO and the electron affinity of the LUMO can be identified based on their respective energies. The HOMO–LUMO gap, also known as the difference in energy between the HOMO and LUMO states, is an essential indicator of dependability. High chemical stability is indicated by a significant HOMO–LUMO gap. The HOMO–LUMO energy hole has also been used to measure activation hardness. Because a smaller energy gap often causes a more straightforward polarization of the molecule, the subjective sense of hardness is inextricably linked with polarizability (Becke, 1993).

2.2.2.3. Dipole moments (μ). The Net molecule polarity, or charge, is measured by the dipole moment. The product of the atom's charge and the distance between the two bound atoms is called the bond strength. A polar covalent bond's dipole moment serves as a gauge for its polarity (Lestari and Indrayanto, 2014). The absolute value of the molecular dipole moment can be determined by adding up the dipole moments of the various bonds in the molecule (Lee et al., 1988).

2.2.2.4. Ionization potential (IP). The amount of energy needed to remove electrons from molecules or atoms in order to an anion (cation) is known as the ionization potential (Yaqo e al., 2020).

$$X + \text{energy} = X^{+} + e$$

The EHOMO's ionization potential may be calculated using the following Eq. (3.1).

$$\text{IE(Ionization potential)} \sim -\text{EHOMO} \tag{3.1}$$

The ionization energy of atoms and molecules is a measure of their chemical reactivity. Atoms and molecules with high ionization energy are more stable, whereas those with low ionization energy are more reactive (Yaqo et al., 2020). Higher activities are from low ionization energy.

2.2.2.5. Electron affinity (EA). When an electron is brought into a system and an antimatter particle is produced, the amount of energy released is referred to as electron affinity (EA) (Yaqo et al., 2020).

$$X + e - = X - + \text{energy}$$

Electron affinity related to ELUMO is shown in Eq. (3.2).

$$\text{EA(Electron affinity)} \sim -\text{ELUMO} \tag{3.2}$$

When reacting with electrophiles, the more reactive molecule has greater HOMO energy, whereas nucleophiles need a lower LUMO energy (Khadom et al., 2021; Kadhim et al., 2021).

2.2.2.6. Chemical hardness (η). The resistance of an atom to a charge transfer is measured by chemical hardness (Peters et al., 1998). Hardness is an imperative property to quantify molecular stability and reactivity. A hard particle has a considerable energy gap (Khadom et al., 2021; Kadhim et al., 2021). It can be calculated by utilizing Eq. (3.3) as follows:

$$\eta(\text{Hardness}) = (\text{IE} - \text{EA})/2 \tag{3.3}$$

2.2.2.7. Chemical softness (S). Chemical softness (S) is the ability of an atom or group of atoms to accept electrons, and it is the inverse of global hardness (Khadom et al., 2021; Kadhim et al., 2021). Softness is a measure the molecular reactivity and stability. Molecules with high values of softness have a small energy gap (Hussein et al., 2020). It is calculated by Eq. (3.4).

$$\text{S(global softness)} = 1/\eta \tag{3.4}$$

2.2.2.8. Electronegativity (χ). In the theory of chemical reactivity, electronegativity is advantageous. Definition: It is the capacity to attract electrons from atoms or a collection of them (Khadom et al., 2021; Kadhim et al., 2021). It is calculated by the following Eq. (3.5):

$$\chi(\text{electronegativity}) = (\text{IE} + \text{EA})/2 \tag{3.5}$$

Table 1
In vitro cell proliferation-inhibitory activity of the synthesized compounds (IC_{50}, μM)[a].

Compound	A549	HeLa	MCF-7
2	> 50	33.6 ± 0.04	> 50
3	> 50	36.4 ± 1.2	> 50
4	**19.4 ± 0.3**	**20.1 ± 0.6**	**21.6 ± 2.2**
5	**15.1 ± 1.9**	**15.6 ± 1.3**	**6.0 ± 0.7**
6	**8.0 ± 1.4**	**9.8 ± 0.8**	**± 0.4**

The derivatives of the significance [bold] showed significant activities against A-549, HeLa and MCF-7 cells.
[a] Values represent means ± SD based on three individual experiments.

2.3. Molecular docking

In the present investigation, software programs such as Molecular Graphic Laboratory (MGL) and Gaussian View were utilized. (09). The geometrical optimization of the compounds using the (6-311G) basis set was proposed by the DFT (Becke, 1993). LDH-5 cancer cells were identified as a prospective target for inhibition by the complexes that are the subject of this study. (Research Collaborator for Structural Bioinformatics) RCSB (Berman et al., 2000). The information necessary to determine the protein's structure was obtained by employing (5NQR). Through the use of autodock tools, each component's LDH-5 and drug locations have been established. (ADT, version 1.5.6). ADT (files with the extension *.pdbqt) can be used to determine the structure of proteins or their complexes. During the process of computing, both polar hydrogen atoms or Gasteiger charges are taken into consideration. In the event that the user does not specify the root of the molecule, it will be determined by the Autodock on its own. Autodock used an automated procedure to choose the root (Hussein et al., 2020) and correctly calculated the atomic affinity maps and electrostatics for every single ligand atomic group using Autogrid (version 4.2.6). Displaying the interactions that take place between the cell & its complexes is the job of the DSV program.

2.4. Drug-Likeness, pharmacokinetics and pharmacodynamics

The computational examination of a drug candidate's bioavailability, pharmacokinetics, and pharmacodynamic toxicity profiles (ADME-Tox) is a crucial prelude to synthesis and in vivo trials (Daoui et al., 2023a). Integrating experimental in vitro tests into a bona fide screening strategy often results in a significant divergence between in vitro assessments and the intended in vivo outcomes, contributing to a relatively diminished success rate for screened molecules as therapeutic agents. Challenges may encompass: incongruence between the structural properties of the molecule and the drug's bioavailability, failure to attain suitable pharmacokinetics, manifestation of undesirable side effects, lethal dose concentration, risk of toxicity, and failure to achieve the therapeutic goal and biological response.

In our current investigation, our focus lies in ascertaining the compatibility of candidate molecules' drug-like attributes with oral bioavailability using Lipinski and Veber bioavailability rules. Furthermore, we evaluate the pharmacokinetic and pharmacodynamic properties (ADME-Tox) of the candidate drug molecules. This examination employs the SwissADME and pKCSM web servers for implementing pharmacophore-based virtual screening (Daina et al., 2017; Pires et al., 2015).

Table 2
^{1}H NMR theoretically and experimentally values of compound 3.

Functional groups	Theoretical values	Experimental values OF ^{1}H NMR
m, 4H, ArH	6.10	6.60
s, 1H, C4-H	5.5	5.83
s, 6H, OMe	3.70	3.77
bs, 8H, 4CH2	2.79	2.82

m: multi; s: single; bs: broad singlet.

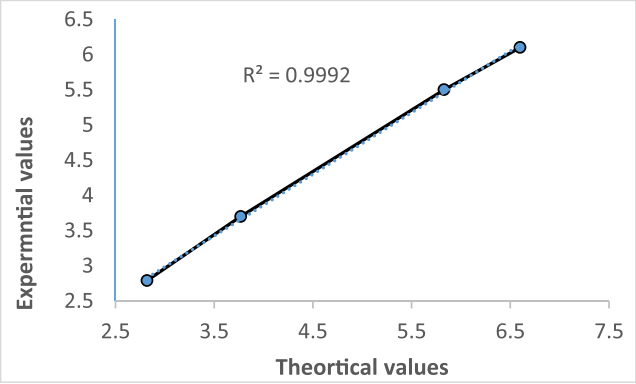

Fig. 3. NMR values in theoretical and experimental study for the compound 3.

3. Results

3.1. Cytotoxic activity

Cytotoxic activity for the compounds including 2, 3, 4, 5, 6 have been investigated and the Table 1 showed the results as follows (Mahal et al., 2017):

3.2. Converge theoretical and experimental results

This part inserts to improve the theoretical values from the experimental according to reference (Hussein et al., 2020). Compound 3 was used as the standard in this study. DFT method and (6-311G) basis set were used to estimate the nuclear magnetic resonance (NMR). The prediction results with experimental shown in Table 2. Fig. 3 included values of R^2 (coefficient of determination). R^2 explains the convergence in two values groups and the best convergence when going to number 1. From this experiment, the R^2 value is (0.9992) in Fig. 3. As a result, the theoretical part of the current study approved the correct estimations.

3.3. Activity and molecular orbitals

These chemicals' action (Khazaal et al., 2020) within the context of the physical characteristics that they possess in this section Table 3. The value of ELUMO drops from 2 to 1, then from 5 to 3 to 4, then ultimately from 4 to 6. The energy gap between the HOMO and LUMO orbitals was discovered to follow the order 1 > 2 > 5 > 3 > 4 > 6, which emphasizes the pattern of activity even more. Ionization energy (IE) is the amount of energy needed to rip an electron out of an atom. To optimize activity, ionization energy has to be below (Allouche et al., 2011). The compounds under investigation are ordered in order of action by the IE: 3 > 6 > 4 > 5 > 1 > 2.

Hardness (Radhi et al., 2020) is a measure of a molecule's reactivity and stability that is represented as the second derivative from the molecule's energy. The sequence is as follows, according to η: 1 > 2 > 5 > 3 > 4 > 6.

The global softness (S) (Radhi et al., 2020) is the quality that opposes the global toughness. The degree of a molecule's softness is one of the most important factors in influencing both its stability and its reactivity. The sequence, according to S, is: 6 > 4 > 3 > 5 > 2 > 1.

When inhibition has a large value, it is more effective for the dipole moment (μ) (Khadom et al., 2021; Kadhim et al., 2021). Hence, the correct series of events is as follows: 2 > 1 > 6 > 3 > 5 > 4. Compounds 1 and 2 were the most active after these circumstances, followed by the compound 6. They will thus consider this in the following section.

Fig. 4 illustrates the distribution of LUMO and HOMO density for the optimized molecules in the gas phase. The color green represents a low electron density, whereas the color red represents an electron density that is elevated (Berman et al., 2000). Metal surfaces with a high electron density have the ability to absorb electrons from atoms in close proximity to them. Electrons are amassed in the Green area of the spectrum. In other words, the division of labor between these two areas is of the utmost importance. The presence of an oxygen atom in the ring is responsible for the increased electron density found at the receptor site for the compound 2. On the other hand, compound 1 appears to attach itself to O atom receptors while simultaneously giving the cell C atoms. In compound 6, the oxygen atom has a similarly high electron density. The receptor site is mainly composed of atoms of carbon and nitrogen.

The compounds have a lower level of action (3, 4 and 5). In the field of computational chemistry, two of the most significant challenges are the optimization of gas-phase molecule morphologies and the estimation of LUMO or HOMO density distributions. These tasks are often performed using quantum chemical methods. A number of different approaches, including as DFT, ab initio methods, or semi-empirical approaches, can be utilized in order to achieve the goal of optimizing the form of a molecule that exists in the gas phase. These methods take into account the electronic structure of the molecule, as well as its geometry, and attempt to find the most stable configuration. In some cases, red is indeed used to represent high electron density, while blue or green is used to represent low electron density. However, in other cases, the colors are reversed or a different color scheme is used altogether Fig. 4.

3.4. TED map of the studies compounds

The compounds 1, 2 and 6 are the ones that are most likely to be found in this area. The total electron density (TED) can be approximated by calculating the number of electrons that are present in a given area. The atoms C and O, which are represented by the color red, are shown to be the most electronegative in the molecules shown in Fig. 5. The color blue comprises a greater number of positive sites, each of which has the ability to take an electron from the donor (Khazaal et al., 2020). The presence of charges has an effect on the physicochemical properties that

Table 3
Quantum chemical characteristics of the molecules in a vacuum.

Comp.	E^{a}_{HOMO}	E^{a}_{LUMO}	IE^{a}	E^{a}_{gap}	η^{a}	S^{b}	μ^{c}
1	−5.63125	−1.67381	5.631251	3.957441	1.978721	0.505377	6.9638
2	−8.26727	−3.81131	8.267278	4.455965	2.227983	0.448837	7.1497
3	−5.42634	−0.31103	5.426345	5.115312	2.557656	0.390983	5.8587
4	−5.50580	−0.22123	5.505804	5.28457	2.642285	0.37846	4.9986
5	−5.57465	−0.59158	5.57465	4.983061	2.491531	0.40136	5.3485
6	−5.47423	−0.08190	5.474238	5.39233	2.696165	0.370897	6.2059

a: in eV, b: in eV^{-1}, c: in Debye.

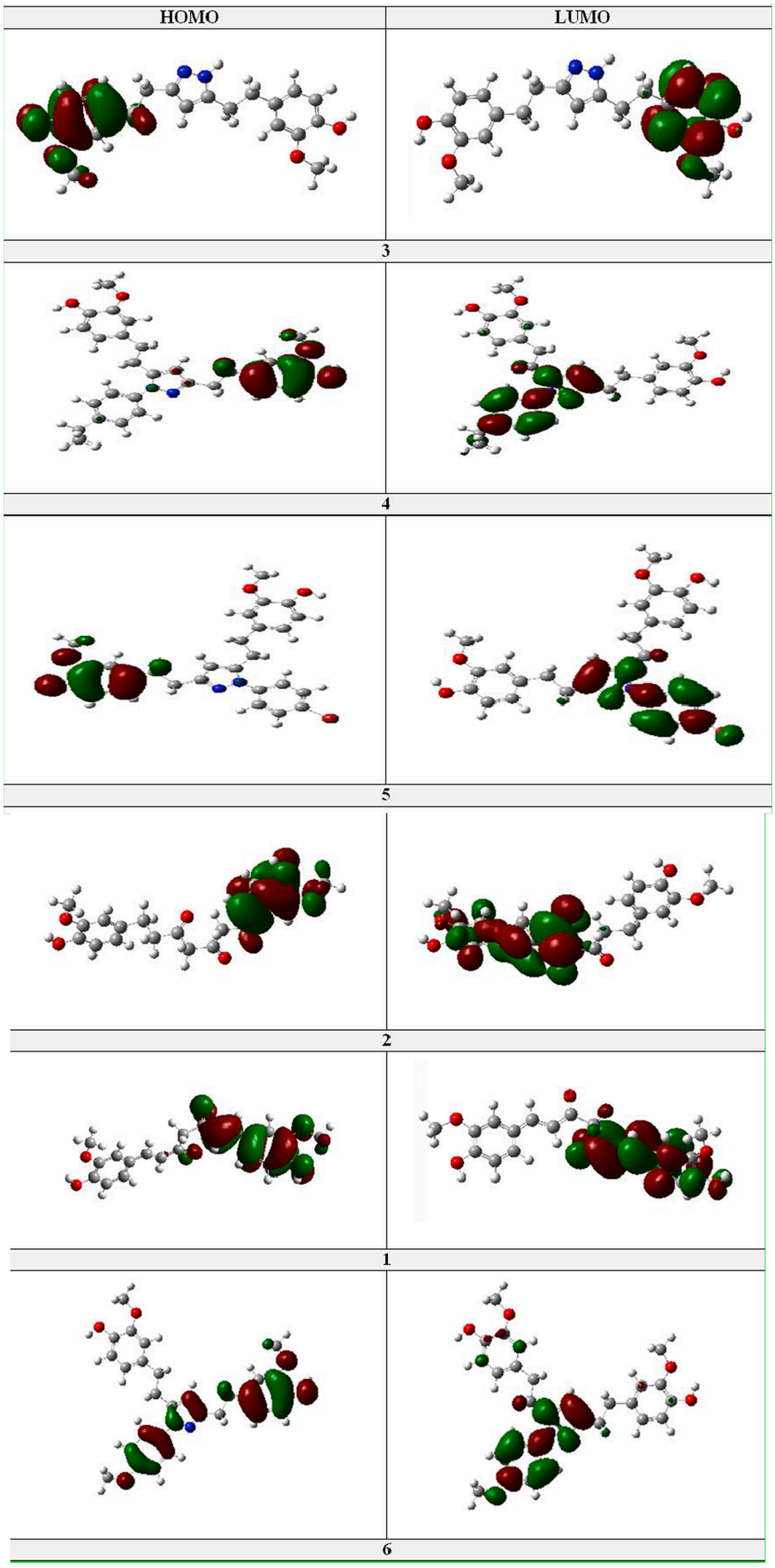

Fig. 4. HOMO-LUMO orbitals of the substances under study.

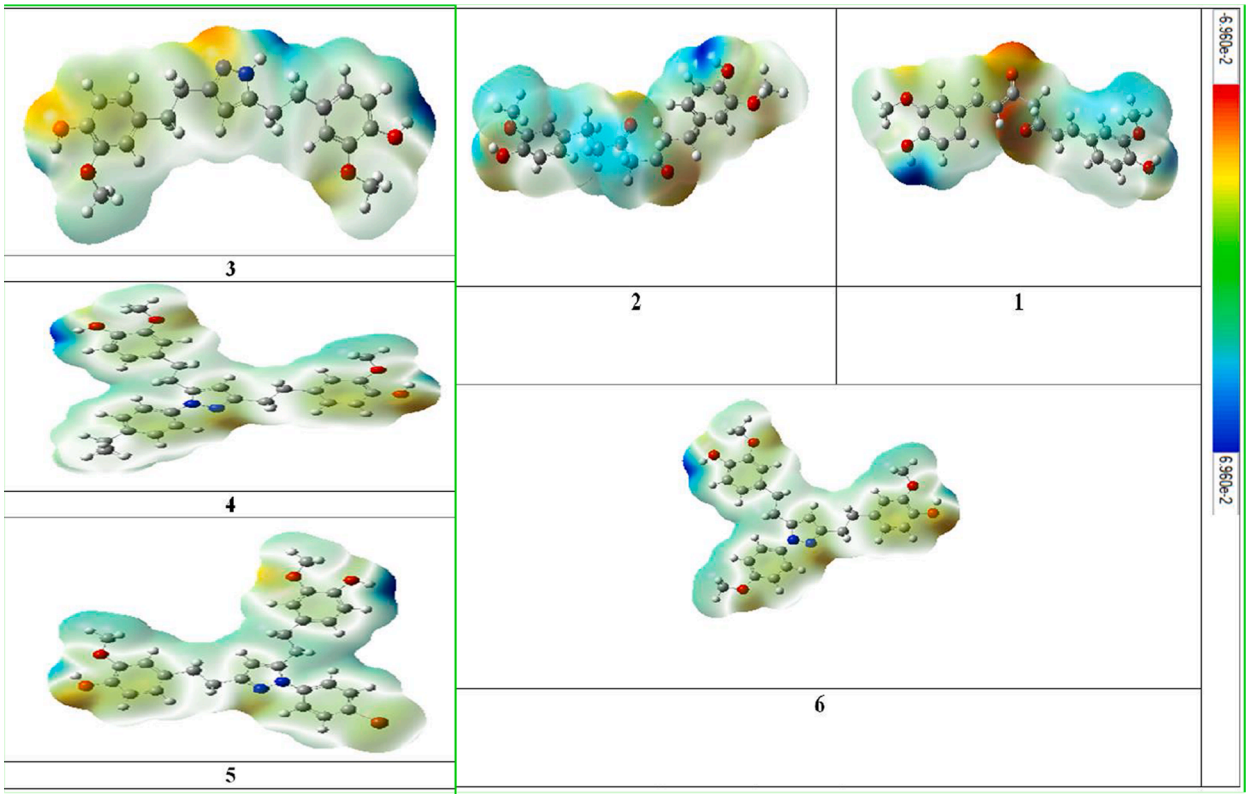

Fig. 5. TED maps of compounds under study.

Table 4
Values for the binding energy and ligand efficiency of the substances under study.

Compound	E_b	L_E
1	−4.24	−0.16
2	−2.86	−0.11
6	−3.52	−0.10
3	−1.59	−0.06
4	−1.89	−0.05
5	−1.46	−0.04

are exhibited by the reactions (Kadhim et al., 2021; Khadom et al., 2021; Yaqo et al., 2020). The electrophilic attack on compounds 1, 2, and 6 showed that the carbon of carbonyl groups, the carbon atom, and the hydrogen atom were the most reactive sites that were able to accept electrons as shown in Fig. 5.

Now the TED of the compounds 3, 4, and 5 in Fig. 5. Some Carbone and Oxygen atoms, the atoms in the molecules with the highest electronegative charge are represented by the color red. In addition, blue contains a greater number of positive sites, which have the potential to absorb donor electrons.

3.5. Molecular docking

The binding energy Eb and the ligand efficiency values of the studied compounds are presented in Table 4.

It has been demonstrated that receptors have active areas that are able to both take in and give out hydrogen bonds. The compounds that were studied contain C atoms that have a donor density of electrons (Fig. 6). These electrons are responsible for the formation of hydrogen bonds. The density, on the other hand, is typically accepted by the other atoms. In addition, the substances that were studied have both hydrophilic and hydrophobic characteristics. Fig. 7 demonstrates that the hydrophilic, represented by the color blue, and the hydrophobic, depicted by the color white, each have unique values.

3.6. Two dimension structures

The most effective compounds 1, 2, and 6 were investigated. Compound 1 contains four different interaction sites when it comes to protein. The linking of the oxygen and hydrogen atoms by a hydrogen bond with (SER, and SYR). In addition, alkyl types, Vander vals, and amide-pi stacking bonds can be discovered Fig. 8.

Whereas compound 2 may have any of the four possible forms of linkages to its constituent parts. Hydrogen bonds between (ASN, SER, and ARG), in addition to a carbon-hydrogen relationship with SER, but the contact with the HIS amino acid is a Vander Waals force.

Furthermore, the linkages in the structures of compounds 2 and 6 are identical, making them structurally equivalent. By three hydrogen bonds with (LYS, GLN, LEU). As can be observed in Fig. 9, the number of linkages in compound 2 is quite high, whereas the number of linkages in compound 6 is not quite (Al-Janabi et al., 2021; Kadhim et al., 2021; Khadom et al., 2021).

The two-dimension intractions of protien with ligands (3, 4, and 5). The N and H atom linkage by a hydrogen bond with (LYS and GLY) and Pi-cation with (LYS) of the compound 3 Fig. 9.

While compound 4 can be found to exist in three different linking forms. Hydrogen bonds to (GLY, LYS), as well as carbon-hydrogen interaction with LYS, whereas LYS is involved in Pi-cation interactions Fig. 9. In addition to this, the structure of compound 5 features a coupling of hydrogen via LYS that has been seen.

3.7. Drug-Likeness, pharmacokinetics and pharmacodynamics

At this screening stage, we have analyzed the bioavailability and pharmacodynamic parameters of the six compounds to pinpoint potential scaffolds for drug design. Table 5 displays the in-silico drug-like property profile acquired for the examined molecules. During this in

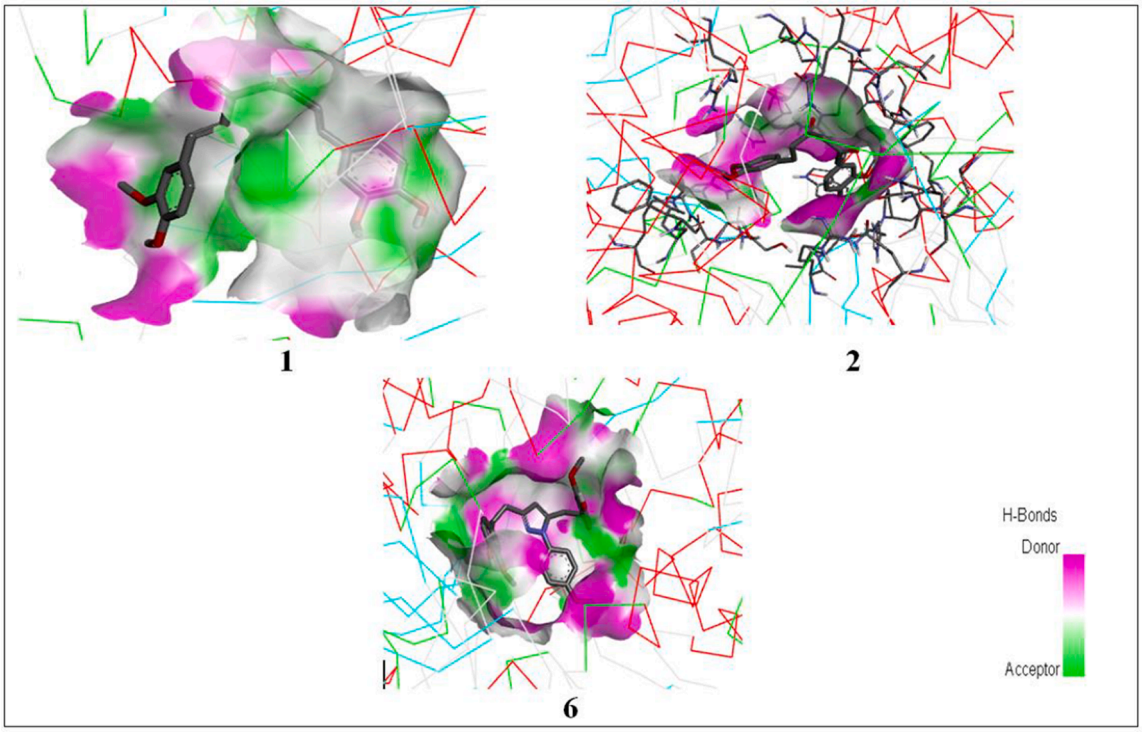

Fig. 6. Sites for forming and accepting H bonds in the spikes' structure.

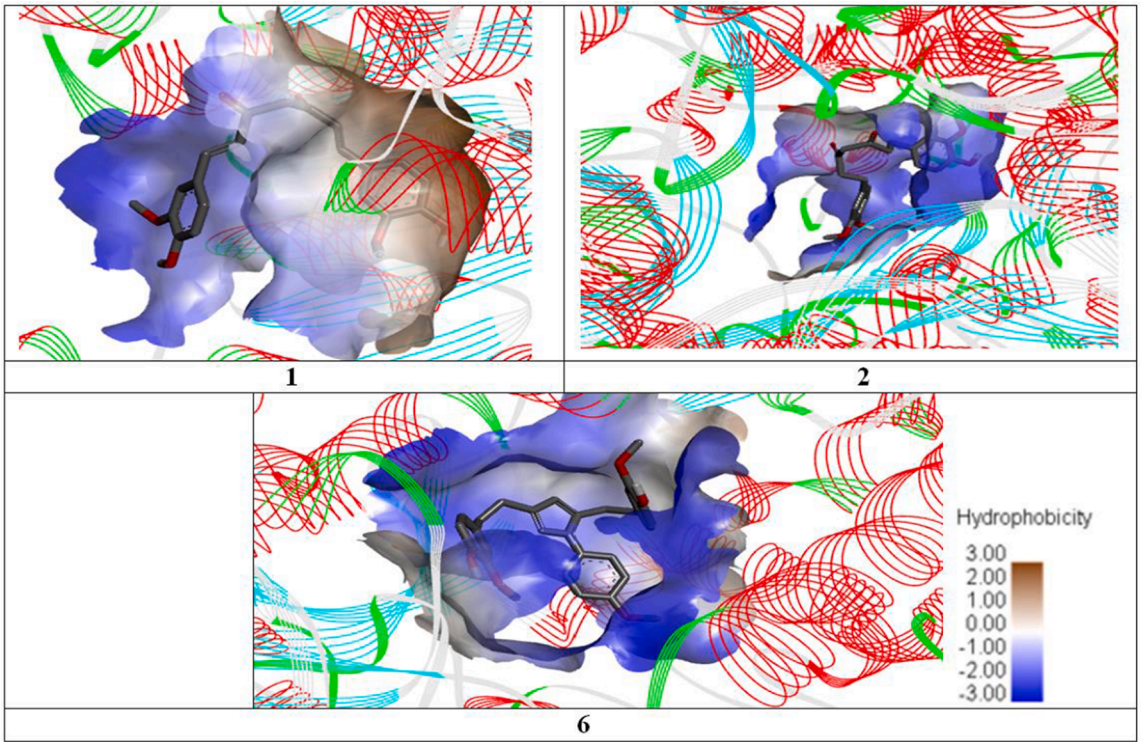

Fig. 7. The connecting region of inhibitors and spikes, respectively, contains hydrophilic and hydrophobic sites.

silico drug-like property screening, we assess bioavailability parameters using Lipinski and Veber rules. Additionally, we examine the in vitro synthetic accessibility index (SA) of the studied molecules.

Furthermore, the absorption assessment reveals that values below 30 % indicate poor absorption in the human intestine, while values above 30 % suggest good absorption capacity (Klantzi et al., 2006). P-glycoprotein, functioning as a drug transporter, regulates drug absorption and flux, expelling foreign substances from the cell (Froom, 2004). Drugs influencing P-glycoprotein may interact with others administered through this pump, potentially yielding opposing effects.

In terms of metabolism, we explored the interactions of cytochrome P450 (CYP) with the six molecules, crucial enzymes for detoxification.

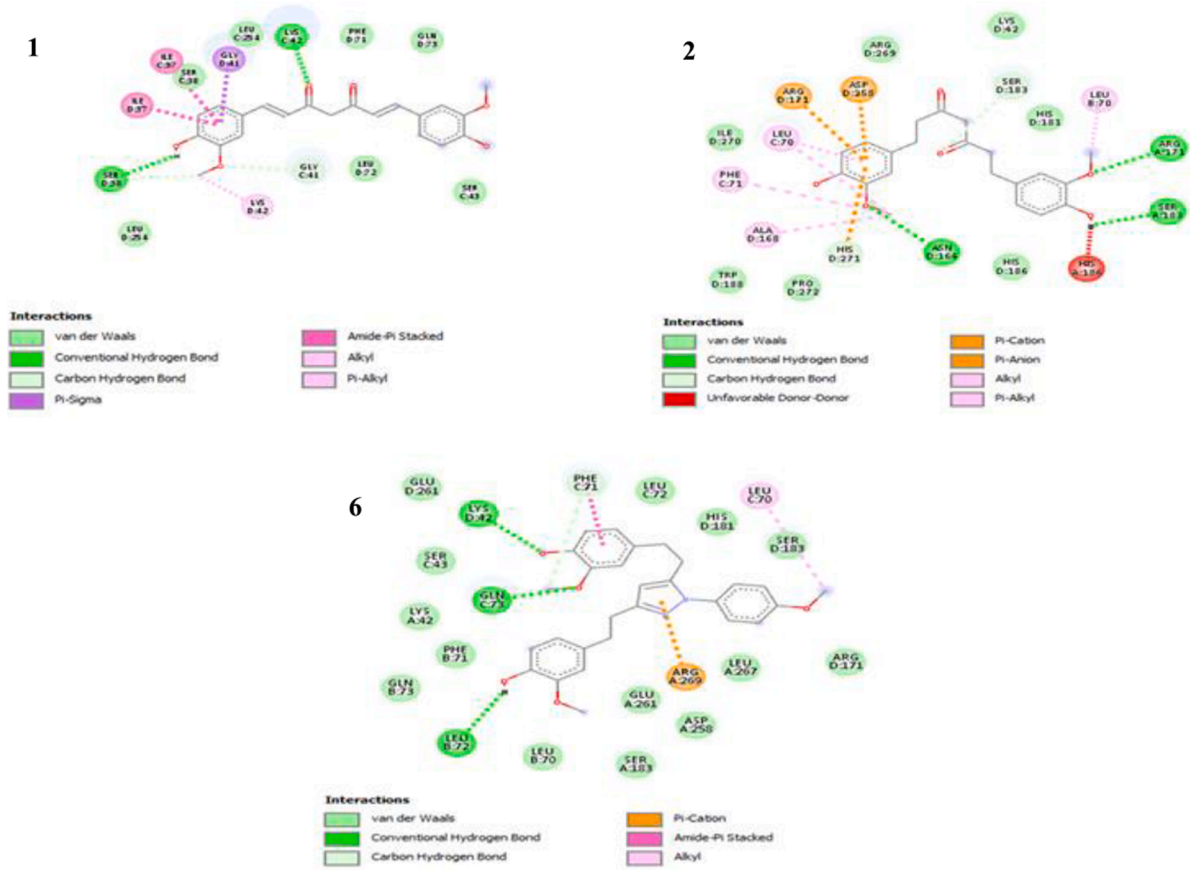

Fig. 8. Two dimensions' structures of the studied compound 1, 2 and 6.

These enzymes oxidize foreign microorganisms to aid in their excretion. Inhibitors of CYP can alter drug metabolism, potentially causing opposite effects. It's crucial to assess molecules' ability to inhibit specific cytochromes, notably 1A2, 2C9, 2C19, 2D6, and 3A4, responsible for over 90 % of drug metabolism (Zanger and Schwab, 2013). Among them, 2D6 and 3A4 play a primary role. Tables 6 and 7 present the ADMET properties profile for the six studied compounds.

4. Discussion

4.1. Anticancer activity

Table 1. show the anticancer activity of the THC and its derivatives 1, 2, 3 and 4 against cancer cell lines including A549, HeLa and MCF-7. The derivatives 2, 3 and 4 showed potent anticancer inhibitory activity with IC_{50} values ranging from 5.9 to 21.6 against all cancer cell lines used compared to the THC (IC_{50} 33.6 - > 50) while compound 1 showed moderate activity (IC_{50} = 33.6) against Hela cell line and weak activity against A549 and MCF-7 cell lines with IC_{50} values of more than 50.

4.2. Molecular docking

Evaluation of the cancer-fighting capabilities of compounds one through six has been completed. Because of the diverse array of substrates that are amenable to being processed by NUDIX hydrolases, this family of nucleotide-metabolizing enzymes has recently been recognized as a significant contributor to the field. NUDT5, often referred to as NUDIX5, has been shown to play a role in the metabolic processes involving ADP-ribose and 8-oxa-guanine. This activity of the protein functions as a rheostat, regulating the expression of hormone-dependent genes and the proliferation of breast cancer cells. In this work, researchers are looking into known NUDT5 substrates to learn more about how NUDT5 influences gene expression and how it helps breast cancer cells grow and spread. This study reveals that NUDT5 is involved in the metabolic process of ADP-ribose, but, it does not show any link to the elimination of oxidized nucleotides from the cell. The finding of potent NUDT5 inhibitors has led to a significant improvement in CETSA's ability to bind to NUDT5 cellular targets. This improvement was made possible as a direct consequence of the discovery of NUDT5 inhibitors. Compounds known as curcuminoids are capable of suppressing the ability of breast cancer cells to create progestin-dependent, PAR-derived nuclear ATP and the processes of chromatin transformation, gene regulation, and proliferation that are directly related to this ability. Our disclosed curcuminoids extract is a highly selective inhibitor of NUDT5 activity and ADP-ribose metabolism that may be used in future studies. The Protein Data Bank ID code used in this study is 5NQR. Binding energy Eb and ligand efficiency LE are two parameters that can be used to describe NUDT5 function in relation to inhibitors. Each of these measurements evaluate a substance's affinity for a receptor protein (receptor) binding energy per atom of ligands. The compounds 1, 2 and 6 have a larger ability to inhibit NUDT5 than the other chemicals do. This can be deduced from the values of their Eb, which are expressed in Kcal/mol Table 4. There is a preferred receptor binding site (L = 1–10) for each of the three substances (1, 2, and 6), with L2 and *L*10 being the most prevalent. The list of substances that follow is presented in the order in which they are most effective at inhibiting LDH-5: 1 > 6 > 2. Furthermore, the Eb and LE of the compounds (3, 4, and 5) presented in Table 4 shown that the harmful compounds act as anti-cancer compounds. The most effective compounds C, THC, and $THCN_3$ were investigated. Compound C contains within it four interaction sites for protein.

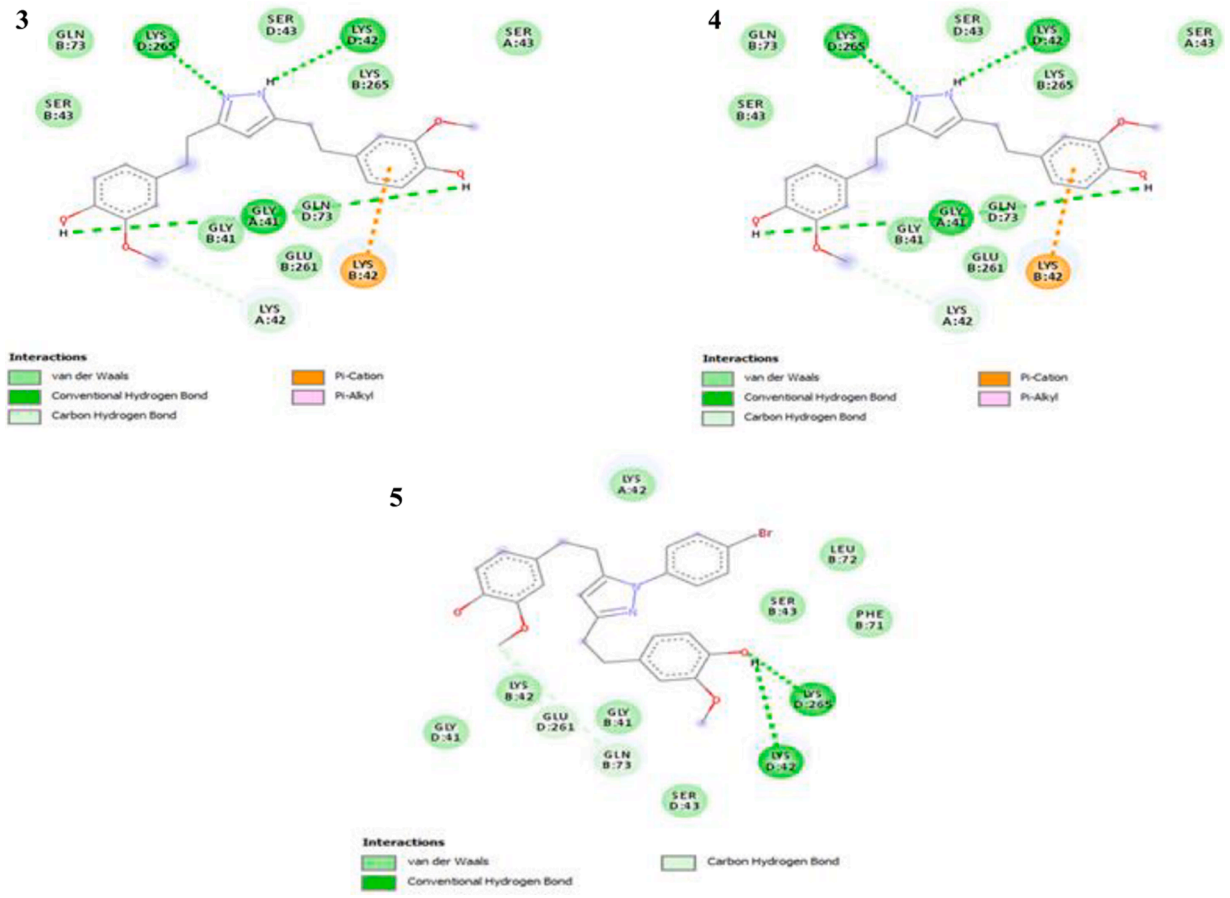

Fig. 9. Two-dimensional structure with interactions of the compound 3, 4 and 5.

Table 5
Drug-like properties profile of the proposed compounds.

Compound	MW (Da)	Log P	nHBA	nHBD	TPSA (Å^2)	nRotB	Drug-likeness		SA
							Lipinski	Veber	
	< 500	≤ 5	< 10	≤ 5	< 140	< 10	Yes/No		0 ≤ SA ≤ 10
1	368.385	3.370	6	2	93.06	8	Yes	Yes	2.97
2	372.417	3.209	6	2	93.06	10	Yes	Yes	2.45
3	368.433	3.409	5	3	87.60	8	Yes	Yes	2.96
4	486.612	5.995	6	2	76.74	10	Yes	Yes	3.85
5	523.427	5.634	6	2	76.74	9	Yes	Yes	3.53
6	474.557	4.880	7	2	85.97	10	Yes	Yes	3.66

MW: Molecular weight; **LogP**: Logarithm of partition coefficient of the compound between n-octanol and water; **nHBA**: Num. H-bond acceptors; **nHBD**: Num. H-bond donors; **TPSA**: Topological Polar Surface Area; **nRotB**: Num. rotatable bonds; **SA:** Synthetic accessibility.

Table 6
Absorption, distribution, excretion and toxicity properties profile predicted in silico.

Compound	Absorption			Distribution		Excretion	Toxicity
	Solubility	HIA	P-Gp	BBB	CNS	TC	AMES
1	Soluble	87.801	Yes	0.041	−3.088	0.080	No
2	Soluble	86.644	Yes	−0.507	−3.203	0.311	No
3	Moderately	90.856	Yes	−1.001	−2.752	0.162	No
4	Poorly	92.910	Yes	−0.460	−2.193	0.356	Yes
5	Poorly	93.433	Yes	−0.660	−2.251	−0.150	No
6	Poorly	96.669	Yes	−0.823	−3.046	0.362	No

HIA: % Human intestinal absorption; **P-Gp**: P-glycoprotein substrate; **VDss**: Human volume of distribution (log L/kg); **BBB**: Blood-Brain-Barrier permeability (log BB); **CNS**: Central nervous system permeability (log PS); **TC**: Total clearance (Log ml/min/kg).

Table 7
Metabolism properties profile predicted in silico.

Compound	Metabolism				
	CYP1A2	CYP2C19	CYP2C9	CYP2D6	CYP3A4
1	No	No	Yes	No	Yes
2	No	No	No	Yes	Yes
3	Yes	Yes	Yes	No	Yes
4	No	Yes	No	Yes	No
5	No	Yes	No	Yes	No
6	No	Yes	No	Yes	No

4.3. Drug-Likeness, pharmacokinetics and pharmacodynamics

Lipinski's rule of five (RO5) physicochemical property standards would be followed by an ideal drug molecule (Abchir et al., 2023). It predicts the drug-likeness of a compound with a specific biological activity that will be administered orally. According to the RO5, a drug-like molecule should have a molecular weight of less than 500 g/mol, a log P value of less than 5, no more than 5 hydrogen bond donors (HBD), and no more than 10 hydrogen bond acceptors (HBA). In addition, according to the Veber rule, a drug-like molecule should have a TPSA of less than 140 Å2 and a nROTB value of less than 10. As depicted in Table 5, none of the compounds violated more than one of the Lipinski's and Veber's rules which is considered acceptable but it warrants careful consideration.

The synthetic accessibility (SA) of the studied compounds is evaluated using the synthetic accessibility index. More SA values are close to 1, very easy to synthesize, while more SA values are close to 10, very difficult and complicated to synthesize (Fukunishi et al., 2014). From the Table 5, we can notice that the synthetic accessibility (SA) values of the examined molecules were between 2.45 and 3.85. This means that all the molecules can be synthesized easily.

Regarding solubility, compounds 1, 2 and 3 exhibit solubility in aqueous mediums, presenting suitable drug-likeness properties for consideration as oral drug candidates. Conversely, compounds 4, 5, and 6 display poor solubility in aqueous mediums.

From Table 6, we can conclude that the six molecules have a high capacity to be absorbed by the intestine in the human body Also, P-glycoprotein substrates, are resistant to metabolism, maintaining their potency and signifying their potential as effective drugs.

Regarding distribution, calculating the Blood-Brain-Barrier (BBB) and central nervous system (CNS) permeabilities allowed us to assess how the tested compounds were distributed in the human body as result, the molecules can't traverse the blood–brain barrier (Table 6).

Molecules with standard BBB permeability values (LogBB < 0.3) and CNS permeability values (LogPS < -2) below the specified thresholds are deemed incapable of penetrating the BBB and central nervous system. The predictions for the distribution indices of the six molecules confirm their suitability for drug use (Daoui et al., 2023b).

In assessing the excretion index, we examined the liver's capacity to filter and excrete toxins using the total clearance index. A lower total clearance value implies greater stability of the drug in the body (Pires et al., 2015). The obtained total clearance values for the molecules indicate that they have low values, suggesting that the designed six-molecule structures are not rapidly excreted. This characteristic implies that these molecules can persist in the body for an extended period, potentially reaching the intended therapeutic target.

The toxicity of the compounds was assessed in silico using the AMES test (Stead et al., 1981). The results of the toxicity evaluation indicated that, with the exception of compound 4, all the molecules are non-toxic.

In terms of metabolism, our findings (Table 7) reveal that the six molecules act as substrates for cytochromes 3A4 or 2C9, without inhibiting all CYP enzymes. This is advantageous, suggesting these compounds lack metabolic interactions with other drugs, reducing the risk of hepatotoxicity and promoting normal metabolism. This lowers the likelihood of side effects, ensuring the drug's proper metabolism and minimizing potential reactions with other medications.

5. Conclusion

An anticancer (breast cancer) role for new compounds 1–6 is proposed. Results from ^{1}HNMR validated $R^{2\prime}$s docking values. DFT studies were carried out to investigate some of the physical properties of the compounds. They proved the high level of activity of the compounds 1, 2 and 6. Based on TED and ESP maps, theoretical simulations predicted that oxygen, nitrogen, and chloride atoms in all of the compounds studied would have the highest electron densities. ADMET analysis suggested favorable oral bioavailability and pharmacokinetics for all studied substances, excluding compound 4. The docking study discusses the compounds' potential as anticancer medications as well as the superior efficacy of the identical molecules 1, 2 and 6, and the least effective inhibitory positions were the compounds 3, 4, and 5. Based on the obtained results from this study, there is ongoing research aim at the development of potent anticancer agents based on the modification of the natural products and study the binding affinity using the molecular docking and employing the DFT calculations to predict the activity stability and electron properties of these compounds leading to more understand the structure of these. Further studies are in progress to invistigate the mechaism of the these compounds and develope more derivatives leading to enhance the anticancer inhibitory activity.

CRediT authorship contribution statement

Ahmed Mahal: Conceptualization, Supervision, Writing – original draft, Writing – review & editing. **Marwan Al-Janabi:** Methodology, Writing – original draft. **Volkan Eyüpoğlu:** Supervision, Writing – original draft. **Anas Alkhouri:** Formal analysis, Resources, Writing – original draft. **Samir Chtita:** Formal analysis, Resources, Writing – original draft. **Mustafa M. Kadhim:** Formal analysis, Resources. **Ahmad J. Obaidullah:** Formal analysis, Resources, Funding acquisition. **Jawaher M. Alotaibi:** Formal analysis, Resources, Funding acquisition. **Xiaoyi Wei:** Formal analysis, Resources. **Mohammad Rizki Fadhil Pratama:** Writing – original draft.

Declaration of competing interest

The authors declare that they have no known competing financial interests or personal relationships that could have appeared to influence the work reported in this paper.

Acknowledgement

The authors acknowledge Cihan University-Erbil, Iraq and Çankırı Karatekin University, Turkey for financial support. The authors extend their appreciation to the Researchers Supporting Project number (RSPD2023R620), King Saud University, Saudi Arabia.

References

Aanouz, I., Belhassan, A., El-Khatabi, K., Lakhlifi, T., El-Idrissi, M., Bouachrine, M., 2021. J. Biomol. Struct. Dyn. 39, 2971–2979. https://doi.org/10.1080/07391102.2020.175879.

Abchir, O., Daoui, O., Nour, H., Yamari, I., Elkhattabi, S., Errougui, A., Chtita, S., 2023. Cannabis constituents as potential candidates for alpha-amylase inhibitor. Sci. Afr. https://doi.org/10.1016/j.sciaf.2023.e01745.

Abdel-Jalil, R.J., Steinbrecher, T., Al-Harthy, T., Mahal, A., Abou-Zied, O.K., Voelter, W., 2015. Stereoselective synthesis and molecular modeling of chiral cyclopentanes. Carbohydr. Res. 415, 12–16. https://doi.org/10.1016/j.carres.2015.07.012.

Ahsan, M.J., Choudhary, K., Ali, A., Ali, A., Azam, F., Almalki, A.H., Tahir, A., 2022. Synthesis, DFT analyses, antiproliferative activity, and molecular docking studies of curcumin analogues. Plants 11 (21), 2835. https://doi.org/10.3390/plants11212835.

Al-Janabi, A.S., Kadhim, M.M., Al-Nassiry, A.I., Yousef, T.A., 2021. Antimicrobial, computational, and molecular docking studies of Zn (II) and Pd (II) complexes

derived from piperidine dithiocarbamate. Appl. Organometallic Chem. 35 (2), e6108 https://doi.org/10.1002/aoc.6108.
Allouche, A.R., 2011. Gabedit—A graphical user interface for computational chemistry softwares. J. Computational Chem. 32 (1), 174–182. https://doi.org/10.1002/jcc.21600.
Baker, M., 2017. Deceptive curcumin offers cautionary tale for chemists. Nature 5 (41), 7636. https://doi.org/10.1038/541144a.
Becke, A.D., 1993. Density-functional thermochemistry. III. The role of exact exchange. J. Chem. Phys. 98, 5648–5652. https://doi.org/10.1063/1.464913.
Berman, H.M., Westbrook, J., Feng, Z., Gilliland, G., Bhat, T.N., Weissig, H., Bourne, P.E., 2000. The protein data bank. Nucl. Acids Res. 28 (1), 235–242. https://doi.org/10.1093/nar/28.1.235.
Cao, W., Chen, X., Chin, Y., Zheng, J., Lim, P.E., Xue, C., Tang, Q., 2022. Identification of curcumin as a potential α-glucosidase and dipeptidyl-peptidase 4 inhibitor: Molecular docking study, in vitro and in vivo biological evaluation. J. Food Biochem. 46 (3) https://doi.org/10.1111/jfbc.13686.
Chen, Z., Nakamura, T., 2004. Statistical evidence for the usefulness of Chinese medicine in the treatment of SARS. Phytotherapy Research: An International Journal Devoted to Pharmacological and Toxicological Evaluation of Natural Product Derivatives 18, 592–594. https://doi.org/10.1002/ptr.1485.
Daina, A., Michielin, O., Zoete, V., 2017. SwissADME: A free web tool to evaluate pharmacokinetics, drug-likeness and medicinal chemistry friendliness of small molecules. Sci. Rep. 7 (1), 42717. https://doi.org/10.1038/srep42717.
Daoui, O., Elkhattabi, S., Chtita, S., 2023a. Design and prediction ADME/Tox properties of novel Magnolol derivatives as anticancer agents for NSCLC using 3D-QSAR. MOLCAD Mol. Docking Stud. Letter Drug Discov. Des. 20 (5), 545–569. https://doi.org/10.2174/1570180819666220510141710.
Daoui, O., Elkhattabi, S., Bakhouch, M., Belaidi, S., Bhandare, R.R., Shaik, A.B., Mali, S. N., Chtita, S., 2023b. A Multi-Step Screening of Small Molecules Based on Cyclohexane-1,3-Dione as Inhibitors of NSCLC by Targeting c-Met Receptor Tyrosine Kinases: discovery and optimization of lead molecules in drug designing. ACS Omega 8 (4), 4294–4319. https://doi.org/10.1021/acsomega.2c07585.
Duan, M., Mahal, A., Mohammed, B., Zhu, Q., Tao, H., Mai, S., Al-Haideri, M., Zhu, Q., 2022. Synthesis and antitumor activity of new tetrahydrocurcumin derivatives via click reaction. Nat. Prod. Res. 36 (20), 5268–5276. https://doi.org/10.1080/14786419.2021.1931181.
El Khatabi, K., Kumar, S., El-Mernissi, R., Singh, A.K., Ajana, M.A., Lakhlifi, T., Bouachrine, M., 2023. J. Biomol. Struct. Dyn. 41, 8402–8416. https://doi.org/10.1080/07391102.2022.2134210.
El-ajaily, M.M., Sarangi, A.K., Mohapatra, R.K., Hassan, S.S., Eldaghare, R.N., Mohapatra, P.K., Raval, M.K., Das, D., Mahal, A., Cipurkovic, A., Al-Noor, T.H., 2019. Transition Metal Complexes of (E)-2 ((2-Hydroxybenzylidene) Amino-3-Mercaptopropanoic Acid: XRD, Anticancer, Molecular Modeling and Molecular Docking Studies. ChemistrySelect 4 (34), 9999–10005. https://doi.org/10.1002/slct.201902306.
El-Barasi, N.M., Miloud, M.M., El-ajaily, M.M., Mohapatra, R.K., Sarangi, A.K., Das, D., Mahal, A., Parhi, P.K., Pintilie, L., Barik, S.R., Bitu, M.N.A., Kudrat-E-Zahan, M., Tabassum, Z., Al-Resayes, S.I., Azam, M., 2020. Synthesis, structural investigations and antimicrobial studies of hydrazone based ternary complexes with Cr (III): Fe (III) and La (III) ions. J. Saudi Chem. Soc. 24 (6), 492–503. https://doi.org/10.1016/j.jscs.2020.04.005.
Eleya, N., Mahal, A., Hein, M., Villinger, A., Langer, P., 2011. Synthesis of Arylated Quinolines by Chemo-and Site-selective Suzuki-Miyaura Reactions of 5, 7-Dibromo-8-(trifluoromethanesulfonyloxy) quinoline. Adv. Synthesis Catal. 353 (14–15), 2761–2774. https://doi.org/10.1002/adsc.201100165.
Esatbeyoglu, T., Huebbe, P., Ernst, I.M., Chin, D., Wagner, A.E., Rimbach, G., 2012. Curcumin—from molecule to biological function. Angewandte Chemieical Int. Ed. 51 (22), 5308–5332. https://doi.org/10.1002/anie.201107724.
Fridlender, M., Kapulnik, Y., Koltai, H., 2015. Plant derived substances with anti-cancer activity: from folklore to practice. Front. Plant Sci. 6, 799. https://doi.org/10.3389/fpls.2015.00799.
Froom, M.F., 2004. Importance of P-glycoprotein at blood-tissue barriers. Trends Pharmacol. Sci. 25 (8), 423–429. https://doi.org/10.1016/j.tips.2004.06.002.
Fukunishi, Y., Kurosawa, T., Mikami, Y., Nakamura, H., 2014. Prediction of synthetic accessibility based on commercially available compound databases. J. Chem. Inf. Model. 54 (12), 3259–3267. https://doi.org/10.1021/ci500568d.
Hussain, I., Yawer, M.A., Appel, B., Sher, M., Mahal, A., Villinger, A., Langer, P., 2008. Synthesis of 4-hydroxy-and 2, 4-dihydroxy-homophthalates by [4+ 2] cycloaddition of 1, 3-bis (silyloxy)-1, 3-butadienes with dimethyl allene-1, 3-dicarboxylate. Tetrahedron 64 (34), 8003–8009. https://doi.org/10.1016/j.tet.2008.05.118.
Hussein, E.A., Shaheed, I.M., Hatam, R.S., Kadhim, M.M., Al-Kadhum, D.T., Abd Al-kareem, E., 2020. Adsorption, thermodynamic and DFT studies of removal RS dye on the Iraqi's clay from aqueous solutions. Syst. Rev. Pharm. 11 (3), 495–502. https://doi.org/10.5530/srp.2020.3.63.
Ibad, M.F., Eleya, N., Obaid-Ur-Rahman, A., Mahal, A., Hussain, M., Villinger, A., Langer, P., 2011. Site-Selective Suzuki-Miyaura Reactions of 1, 4-and 3, 5-Bis (trifluoromethylsulfonyloxy)-2-naphthoates. Synthesis 2011 (13), 2101–2116. https://doi.org/10.1055/s-0030-1260054.
Kadhim, M.M., Salman, A.W., Zarzoor, A.M., Kadhum, W.R., 2021. Inhibition of SARS-CoV-2 reproduction using Boswellia carterii: A theoretical study. J. Mol. Liquids 337, 116440. https://doi.org/10.1016/j.molliq.2021.116978.
Kamel, F.H., Fathulla, C.N., Mahal, A., Alkhouri, A., Rahman, S.E., Osman, A.S., 2022a. Antibacterial activity of *Cassia angustifolia*. Vahl (*Sinameki*) leaf extract against some pathogenic bacteria. Eurasian Chem. Commun. 4, 1108–1114. https://doi.org/10.22034/ecc.2022.344320.1475.
Kamel, F., Sabir, S., Mahal, A., Wei, X., 2022b. In vitro Antibacterial activity of orange peel oil extract from citrus sinensis fruit in Erbil. Egypt. J. Chem 65 (4), 157–160. https://doi.org/10.21608/EJCHEM.2021.93484.4416.
Karthikesan, K., Pari, L., Menon, V.P., 2010. Protective effect of tetrahydrocurcumin and chlorogenic acid against streptozotocin–nicotinamide generated oxidative stress induced diabetes. J. Funct. Foods 2, 134–142. https://doi.org/10.1016/j.jff.2010.04.001.
Khadom, A.A., Kadhim, M.M., Anaee, R.A., Mahood, H.B., Mahdi, M.S., Salman, A.W., 2021. Theoritical evaluation of Citrus Aurantium leaf extract as green inhibitor for chemical and biological corrosion of mild steel in acidic solution: statistical, molecular dynamics, docking, and quantum mechanics study. J. Mol. Liquids 343, 116978. https://doi.org/10.1016/j.molliq.2021.116978.
Khazaal, F.A., Kadhim, M.M., Husseein, H.F., Abbas, Z.M., Hamzah, M.S., Khudhair, I.A., Saieed, H.S., 2020. Electronic transfers and (nlo) properties predicted by ab initio methods with prove experimentally. Neuro Quantol. 18 (1), 46. https://doi.org/10.14704/nq.2020.18.1.NQ20106.
Kim, J.M., Araki, S., Kim, D.J., Park, C.B., Takasuka, N., Baba-Toriyama, H., Tsuda, H., 1998. Chemopreventive effects of carotenoids and curcumins on mouse colon carcinogenesis after 1, 2-dimethylhydrazine initiation. Carcinogenesis 19 (1), 81–85. https://doi.org/10.1093/carcin/19.1.81.
Kim, J.E., Kim, H.R., Kim, J.C., Lee, E.S., Chung, C.H., Lee, E.Y., Chung, B.Y., 2021. Tetrahydrocurcumin ameliorates skin inflamma-tion by modulating autophagy in high-fat diet-induced obese mice. Biomed. Res. Int. 2021 (6621027), 637. https://doi.org/10.1155/2021/6621027.
Klantzi, L., Goumas, K., Kalioras, V., Abrahamsson, B., Dressman, J.B., Reppas, C., 2006. Characterization of the human upper gastro-intestinal contents under conditions simulating bioavailability/bioequivalence studies. Pharm. Res. 23 (1), 165–176. https://doi.org/10.1007/s11095-005-8476-1.
Kondhare, D., Deshmukh, S., Lade, H., 2019. Curcumin analogues with aldose reductase inhibitory activity: synthesis, biological evaluation, and molecular docking. Processes 7 (7), 417. https://doi.org/10.3390/pr7070417.
Lakhan, S.E., Ford, C.T., Tepper, D., 2015. Zingiberaceae extracts for pain: a systematic review and meta-analysis. Nutr. J. 14 (1), 1–10. https://doi.org/10.1186/s12937-015-0038-8.
Lee, C., Yang, W., Parr, R.G., 1988. Development of the Colle-Salvetti correlation-energy formula into a functional of the electron density. Phys. Rev. 37 (2) https://doi.org/10.1103/PhysRevB.37.785.
Lestari, M.L., Indrayanto, G. 2014. Curcumin. Profiles of Drug Substances, Excipients and Related Methodology, 39: 113-204. https://doi.org/10.1016/B978-0-12-800173-8.00003-9.
Li, L., Liu, X., Li, S., Wang, Q., Wang, H., Xu, M., An, Y., 2021. Tetrahydrocurcumin protects against sepsis-induced acute kidney injury via the SIRT1 pathway. Ren. Fail. 43, 1028–1040. https://doi.org/10.1080/0886022x.2021.1942915.
Limtrakul, P., Chearwae, W., Shukla, S., Phisalphong, C., Ambudkar, S.V., 2007. Modulation of function of three ABC drug transporters, P-glycoprotein (ABCB1): mitoxantrone resistance protein (ABCG2) and multidrug resistance protein 1 (ABCC1) by tetrahydrocurcumin, a major metabolite of curcumin. Mol. Cellular Biochem. 296, 85–95. https://doi.org/10.1007/s11010-006-9302-8.
Mahal, A., Villinger, A., Langer, P., 2010. Synthesis of 1, 2-diarylanthraquinones by site-selective Suzuki-Miyaura reactions of the bis (triflate) of alizarin. Synlett 2010 (07), 1085–1088. https://doi.org/10.1055/s-0029-1219586.
Mahal, A., Villinger, A., Langer, P., 2011. Site-Selective arylation of alizarin and purpurin based on suzuki-miyaura cross-coupling reactions. Eur. J. Org. Chem. 2011 (11), 2075–2087. https://doi.org/10.1002/ejoc.201001497.
Mahal, A., 2015a. Oxetanes as versatile building blocks in the total synthesis of natural products: an overview. Eur. J. Chem. 6 (3), 357–366. https://doi.org/10.5155/eurjchem.6.3.357-366.1267.
Mahal, A., Abu-El-Halawa, R., Zabin, S.A., Ibrahim, M., Al-Refai, M., Kaimari, T., 2015b. Synthesis, characterization and antifungal activity of some metal complexes derived from quinoxaloylhydrazone. World J. Org. Chem. 3 (1), 1–8. https://doi.org/10.12691/wjoc-3-1-1.
Mahal, A., D'Errico, S., Borbone, N., Pinto, B., Secondo, A., Costantino, V., Piccialli, G., 2015c. Synthesis of cyclic N1-pentylinosine phosphate, a new structurally reduced cADPR analogue with calcium-mobilizing activity on PC12 cells. Beilstein J. Org. Chem. 11 (1), 2689–2695. https://doi.org/10.3762/bjoc.11.289.
Mahal, A., Wu, P., Jiang, Z.H., Wei, X., 2017. Synthesis and cytotoxic activity of novel tetrahydrocurcumin derivatives bearing pyrazole moiety. Nat. Prod. Bioprospect. 7, 461–469. https://doi.org/10.1007/s13659-017-0143-9.
Mahal, A., Wu, P., Jiang, Z.H., Wei, X., 2019. Schiff bases of tetrahydrocurcumin as potential anticancer agents. ChemistrySelect 4 (1), 366–369. https://doi.org/10.1002/slct.201803159.
Mahal, A., Duan, M., Zinad, D.S., Mohapatra, R.K., Obaidullah, A.J., Wei, X., Pradhan, M. K., Das, D., Kandi, V., Zinad, H.S., Zhu, Q., 2021. Recent progress in chemical approaches for the development of novel neuraminidase inhibitors. RSC. Adv. 11, 1804–1840. https://doi.org/10.1039/D0RA07283D.
Manolova, Y., Deneva, V., Antonov, L., Drakalska, E., Momekova, D., Lambov, N., 2014. The effect of the water on the curcumin tautomerism: a quantitative approach. Spectrochimica Acta Part a: Mol. Biomol. Spectrosc. 132, 815–820. https://doi.org/10.1016/j.saa.2014.05.096.
Marzano, M., Terracciano, M., Piccialli, V., Mahal, A., Nilo, R., D'Errico, S., 2022. O6-[(2″, 3″-O-Isopropylidene-5″-O-t butyldimethylsilyl) pentyl]-5′-O-t butyldiphenylsilyl-2′, 3′-O-isopropylideneinosine. Molbank 2022 (1), M1345. https://doi.org/10.3390/M1345.
Mohapatra, R.K., El-ajaily, M.M., Alassbaly, F.S., Sarangi, A.K., Das, D., Maihu, A.A., Ben-Gweirif, S.F., Mahal, A., Suleiman, M., Perekhoda, L., Azam, M., Al-Noor, T.H., 2021. DFT, anticancer, antioxidant and molecular docking investigations of some ternary

Ni (II) complexes with 2-[(E)-[4-(dimethylamino) phenyl] methyleneamino] phenol. Chem. Papers 75, 1005–1019. https://doi.org/10.1007/s11696-020-01342-8.
Nelson, K.M., Dahlin, J.L., Bisson, J., Graham, J., Pauli, G.F., Walters, M.A., 2017. The essential medicinal chemistry of curcumin: miniperspective. J. Medicinal Chem. 60 (5), 1620–1637. https://doi.org/10.1021/acs.jmedchem.6b00975.
Pari, L., Amali, D.R., 2005. Protective role of tetrahydrocurcumin (THC) an active principle of turmeric on chloroquine induced hepatotoxicity in rats. J. Pharm Pharma Sci. 8 (1), 115–123.
Peters, J.W., Lanzilotta, W.N., Lemon, B.J., Seefeldt, L.C., 1998. X-ray crystal structure of the Fe-only hydrogenase (CpI) from Clostridium pasteurianum to 1.8 angstrom resolution. Science 282 (5395), 1853–1858. https://doi.org/10.1126/science.282.5395.1853.
Pires, D.E., Blundell, T.L., Ascher, D.B., 2015. pkCSM: Predicting small-molecule pharmacokinetic and toxicity properties using graph-based signatures. J. Med. Chem. 58 (9), 4066–4072. https://doi.org/10.1021/acs.jmedchem.5b00104.
Plata, R.E., Singleton, D.A., 2015. A case study of the mechanism of alcohol-mediated Morita Baylis-Hillman reactions. The importance of experimental observations. J. Am. Chem. Soc. 137 (11), 3811–3826. https://doi.org/10.1021/ja5111392.
Radhi, A.H., Du, E.A., Khazaal, F.A., Abbas, Z.M., Aljelawi, O.H., Hamadan, S.D., Kadhim, M.M., 2020. HOMO-LUMO energies and geometrical structures effecton corrosion inhibition for organic compounds predict by DFT and PM3 methods. Neuro Quantol. 18 (1), 37. https://doi.org/10.14704/nq.2020.18.1.NQ20105.
Saeed, M.E., Yücer, R., Dawood, M., Hegazy, M.E.F., Drif, A., Ooko, E., Efferth, T., 2022. In silico and in vitro screening of 50 Curcumin compounds as EGFR and NF-κB inhibitors. Int. J. Mol. Sci. 23 (7), 3966. https://doi.org/10.3390/ijms23073966.
Salman, A.W., Haque, R.A., Kadhim, M.M., Malan, F.P., Ramasami, P., 2019. Novel triazine-functionalized tetra-imidazolium hexafluorophosphate salt: Synthesis, crystal structure and DFT study. J. Mole. Str. 1198, 126902 https://doi.org/10.1016/j.molstruc.2019.126902.
Salman, G.A., Mahal, A., Shkoor, M., Hussain, M., Villinger, A., Langer, P., 2011. Regioselective Suzuki-Miyaura reactions of the bis (triflate) of 1, 2, 3, 4-tetrahydro-9, 10-dihydroxyanthracen-1-one. Tetrahedron Lett. 52 (3), 392–394. https://doi.org/10.1016/j.tetlet.2010.11.052.
Salman, G.A., Zinad, D.S., Mahal, A., 2020. Design, synthesis, and biological evaluation of new quinoline-based heterocyclic derivatives as novel antibacterial agents. Monatsh. Chem. 151, 1621–1628. https://doi.org/10.1007/s00706-020-02686-3.
Salman, G., Zinad, S., Mahal, A., Rizki, A., Fadhil Pratama, M., Duan, M., Alkhouri, A., Alamiery, A., 2022. Synthesis, antibacterial activity, and molecular docking study of bispyrazole-based derivatives as potential antibacterial agents. ChemistrySelect 7 (4), e202103901. https://doi.org/10.1002/slct.202103901.
Sayin, K., Kariper, S.E., Taştan, M., Sayin, T.A., Karakaş, D., 2019. Investigations of structural, spectral, electronic and biological properties of N-heterocyclic carbene Ag (I) and Pd (II) complexes. J. Mol. Struct. 1176, 478–487. https://doi.org/10.1016/j.molstruc.2018.08.103.
Song, G., Lu, H., Chen, F., Wang, Y., Fan, W., Shao, W., Lin, B., 2018. Tetrahydrocurcumin-induced autophagy via suppression of PI3K/Akt/mTOR in non-small cell lung carcinoma cells. Mol. Med. Rep. 17 (4), 5964–5969. https://doi.org/10.3892/mmr.2018.8600.
Soudani, W., Zaki, H., Alaqarbeh, M., ELMchichi, L., Bouachrine, M., Hadjadj-Aoul, F.Z., 2023. Discover the medication potential of algerian medicinal plants against Sars-Cov-2 Main Protease (M^{pro}): molecular docking, molecular dynamic simulation, and ADMET analysis. ChemistryAfrica. https://doi.org/10.1007/s42250-023-00684-6.
Stead, A.G., Hasselblad, V., Creason, J.P., Claxton, L., 1981. Modeling the Ames test. Mutat. Res. 85 (1), 13–27. https://doi.org/10.1016/0165-1161(81)90282-X.
Velasco, G., Hernández-Tiedra, S., Dávila, D., Lorente, M., 2015. The use of cannabinoids as anticancer agents. Prog. Neuropsychopharmacol. Biol. Psychiatry 64, 259–266. https://doi.org/10.1016/j.pnpbp.2015.05.010.
Wani, M.C., Taylor, H.L., Wall, M.E., Coggon, P., Mcphail, A.T., 1971. Plant antitumor agents. VI. Isolation and structure of taxol, a novel antileukemic and antitumor agent from *Taxus brevifolia*. J. Am. Chem. Soc. 93, 2325–2327. https://doi.org/10.1021/ja00738a045.
Wilken, R., Veena, M.S., Wang, M.B., Srivatsan, E.S., 2011. Curcumin: a review of anti-cancer properties and therapeutic activity in head and neck squamous cell carcinoma. Mol. Cancer 10 (1), 1–19. https://doi.org/10.1186/1476-4598-10-12.
Yang, L., Mahal, A., Liu, Y., Li, H., Wu, P., Xue, J., Wei, X., 2017. Two new 2, 5-diketopiperazines produced by Streptomyces sp. SC0581. Phytochem. Lett. 20, 89–92. https://doi.org/10.1016/j.phytol.2017.04.012.
Yang, L., Li, H., Wu, P., Mahal, A., Xue, J., Xu, L., Wei, X., 2018. Dinghupeptins a–d, chymotrypsin inhibitory cyclodepsipeptides produced by a soil-derived streptomyces. J. Natural Products 81 (9), 1928–1936. https://doi.org/10.1021/acs.jnatprod.7b01009.
Yaqo, E.A., Anaee, R.A., Abdulmajeed, M.H., Tomi, I.H.R., Kadhim, M.M., 2020. Electrochemical, morphological and theoretical studies of an oxadiazole derivative as an anti-corrosive agent for kerosene reservoirs in Iraqi refineries. Chem. Papers 74 (6), 1739–1757. https://doi.org/10.1007/s11696-019-01022-2.
Zanger, U.M., Schwab, M., 2013. Cytochrome P450 enzymes in drug metabolism: regulation of gene expression, enzyme activities, and impact of genetic variation. Pharmacol. Ther. 138 (1), 103–141. https://doi.org/10.1016/j.pharmthera.2012.12.007.
Zhao, F., Gong, Y., Hu, Y., Lu, M., Wang, J., Dong, J., Chen, D., Chen, L., Fu, F., Qiu, F., 2015. Curcumin and its major metabolites inhibit the inflammatory response induced by lipopolysaccharide: Translocation of nuclear factor-κB as potential target. Mol. Med. Rep. 11, 3087–3093. https://doi.org/10.3892/mmr.2014.3079.
Zinad, D.S., Mahal, A., Al-Amiery, A., 2020a. An efficient synthesis of novel imidazo-aminopyridinyl derivatives from 2-chloro-4-cyanopyridine. Org. Prep. Proced. Int. 52 (4), 361–367. https://doi.org/10.1080/00304948.2020.1767491.
Zinad, D.S., Mahal, A., Shareef, O.A., 2020b. Antifungal activity and theoretical study of synthesized pyrazole-imidazole hybrids. IOP Conf. Ser.: Mater. Sci. Eng. 770 (1), 012053 https://doi.org/10.1088/1757-899X/770/1/012053.
Zinad, D.S., Mahal, A., Mohapatra, R.K., Sarangi, A.K., Pratama, M.R.F., 2020c. Medicinal chemistry of oxazines as promising agents in drug discovery. Chem. Biol. Drug Des. 95 (1), 16–47. https://doi.org/10.1111/cbdd.13633.
Zinad, D.S., Shareef, O.A., Mahal, A., 2020d. Theoretical investigation for synthesis and characterization of two novel disubstituted imidazoles using microwave. AIP Conf. Proc. 2213 (1), 020188 https://doi.org/10.1063/5.0000128.
Zinad, D.S., Mahal, A., Salman, G.A., 2021a. Synthesis and antibacterial activity of novel 1, 3-oxazine derivatives. Org. Prep. Proced. Int. 53 (6), 578–584. https://doi.org/10.1080/00304948.2021.1975486.
Zinad, D.S., Mahal, A., Siswodihardjo, S., Pratama, M.R.F., Mohapatra, R., 2021b. 3D-molecular modeling, antibacterial activity and molecular docking studies of some imidazole derivatives. Egypt. J. Chem. 64 (1), 93–105. https://doi.org/10.21608/EJCHEM.2020.31043.2662.
Zinad, D.S., Mahal, A., Salman, G.A., Shareef, O.A., Pratama, M.R.F., 2022. Molecular docking and DFT study of synthesized oxazine derivatives. Egypt. J. Chem. 65 (7), 231–240. https://doi.org/10.21608/EJCHEM.2021.102664.4755.
Zinad, D.S., Salman, G.A., Mahal, A., Hussein, F.H., 2023a. Molecular modeling study and antifungal activity of some synthesized quinoline derivatives. AIP Conf. Proc. 2457 (1), 030001 https://doi.org/10.1063/5.0118611.
Zinad, D.S., Mahal, A., Salman, G.A., Alduhan, I.A., Yahya, M., Meito, D., Alkhouri, A., Zinad, Y.S., 2023b. Synthesis of novel quinolines with antibacterial activity. Org. Prep. Proced. Int. https://doi.org/10.1080/00304948.2023.2238099.